ELSEVIER

Catalysis Today 58 (2000) 141–149

CATALYSIS TODAY

www.elsevier.com/locate/cattod

Photocatalytic behavior of mixed WO_3/WS_2 powders

A. Di Paola, L. Palmisano*, V. Augugliaro

Dipartimento di Ingegneria Chimica dei Processi e dei Materiali, Università di Palermo, Viale delle Scienze, 90128 Palermo, Italy

Abstract

Polycrystalline mixed WO_3/WS_2 powders have been prepared by different methods. The samples have been characterized by bulk and surface techniques and tested as catalysts for the photodegradation of phenol. The results have indicated that the coupling of WO_3 and WS_2 leads to an enhanced rate of disappearance of the organic substrate. The effect is explained as the result of the simultaneous electron transfer from WS_2 to WO_3 and hole transfer from WO_3 to WS_2. The efficiency of the mixed WO_3/WS_2 systems strongly depends on the relative amounts of WO_3 and WS_2 in the various samples. A maximum of photoactivity is obtained when the surface WS_2 and WO_3 molar fraction is about 0.5. © 2000 Elsevier Science B.V. All rights reserved.

Keywords: Coupled semiconductors; WO_3/WS_2; Phenol photooxidation

1. Introduction

Photocatalytic reactions on semiconductor powders are of great interest because of their applicability to the treatment of a large variety of pollutants [1,2]. Upon band gap excitation photoinduced electrons and holes can reduce and oxidize species adsorbed on the semiconductor particles, but one disadvantage of the particulate systems is the high degree of recombination between the photogenerated charge carriers.

An efficient charge separation can be obtained by employing photocatalysts obtained by coupling two different semiconductor phases [3–6]. The effect is explained as a result of a vectorial transfer of electrons and holes from a semiconductor to another: when both semiconductors are illuminated, electrons accumulate at the lower-lying conduction band of one semiconductor while holes accumulate at the valence band of the other compound [5,6]. These processes of charge separation are very fast and the efficiency of reduction or oxidation of the adsorbed substrate remarkably increases.

A large variety of coupled semiconductor systems has been so far studied [3–26]. Most of them consisted of a mechanical mixture of polycrystalline or colloidal semiconductors suspended in water [3–21]. Mixed particles supported on Nafion [11], silica [12–13] or alumina [14] or films obtained by deposition of colloidal semiconductors on optically transparent electrodes have also been employed [22–26].

Recently, polycrystalline mixed WO_3/WS_2 systems have been prepared and successfully tested [27–29]. Unlike other coupled semiconductor systems, the enhanced photoactivity of these samples is not due to a simple mixture of two semiconductors with different energy levels but to the coexistence of WO_3 and WS_2 in the same particle. The study of the structural properties of these catalysts seems important to understand the possible employment of other different oxide/sulfide systems in heterogeneous photocatalysis. The present paper reports on the preparation and characterization of mixed WO_3/WS_2 powders obtained by

---

* Corresponding author. Tel.: +39-091-656-7215;
fax: +39-091-599-766.
E-mail address: palmisan@dicpm.unipa.it (L. Palmisano)

PII: S0920-5861(00)00249-2

different methods. The samples were characterized by X-ray diffraction, determination of specific surface area, diffuse reflectance spectroscopy, scanning electron microscopy (SEM) and X-ray photoelectron spectroscopy (XPS) analysis. The photodegradation of phenol has been used to examine the photocatalytic behavior of the powders.

2. Experimental

Different mixed WS_2/WO_3 systems were prepared by oxidation of WS_2 or by sulfidation of WO_3, as follows:

1. WS_2 (Aldrich) was placed in a cylindrical Pyrex reactor and allowed to react with a flux of air at different temperatures and for different times;
2. commercial WO_3 (Carlo Erba) or WO_3 powder obtained by decomposition of ammonium metatungstate $(NH_4)_6H_2W_{12}O_{41}$ (Fluka) in air at 823 K for 16 h, were sulfidized by a flux of gaseous H_2S (Praxair) in the same experimental conditions as in 1. Samples with a high surface area were prepared by wet impregnation of γ-Al_2O_3 (Fluka) with an aqueous solution of ammonium meta-tungstate. The powders were dried in air at 393 K for 16 h, calcined in air at 823 K for 16 h and subsequently sulfidized with H_2S. Samples with high amounts of WO_3 were obtained by repeated impregnation steps.

The samples were denoted by three numbers, e.g. 673/1/6, which identify the temperature (K), the time of oxidation (h) and the amount of initial powder (g), respectively. A label (ox, sulf) indicates the preparation method.

The composition of the mixed powders was gravimetrically determined by calcining the samples in air at 873 K for 3 h. The sulfur content was calculated from the weight loss, assuming WO_3 as the only product of calcination.

X-ray diffraction patterns were obtained using a Philips diffractometer with a Ni-filtered Cu Kα radiation and the 2θ scan rate was $2^\circ\,\mathrm{min}^{-1}$. The specific surface areas were measured by the single-point BET method using a Micromeritics Flow Sorb 2300 apparatus. Diffuse reflectance spectra were obtained in air at room temperature, in the range 200–500 nm, by means of a Varian DMS 90 UV–Vis spectrophotometer using $BaSO_4$ as the reference sample. SEM observations were performed by means of a Philips 505 microscope, operating at 25 kV and equipped with an electron microprobe used in an energy dispersive mode (EDX) to obtain quantitative information on the distribution of WO_3 and WS_2 in the samples.

XPS spectra were recorded with a Perkin Elmer PHI 5600-ci spectrometer using a standard Al Kα source (1486.6 eV) working at 300 W. The working pressure was around 1×10^{-6} Pa. As an internal reference for the absolute binding energies, the C 1s peak of hydrocarbon contamination set at 248.8 eV was used. The atomic composition was evaluated using PHI sensitivity factors [29]. The samples were analyzed as pellets after being ground in a mortar. WS_2 (Aldrich) and WO_3 (Carlo Erba) were analyzed as reference compounds.

A 1.5 l batch cylindrical Pyrex reactor was used for the photocatalytic experiments. The irradiation source was a 1000 W medium-pressure Hg lamp (Helios Italquartz) equipped with a water jacket to eliminate IR radiations. The photon flux emitted by the lamp was $22\,\mathrm{mW\,cm^{-2}}$. The reaction mixture contained $1.5\,\mathrm{g\,l^{-1}}$ of powder and a 200 mM aqueous phenol solution (pH=4.5). The suspension was magnetically stirred and oxygen was continuously bubbled before and during the irradiation.

Samples of 10 ml volume were withdrawn from the suspension at fixed intervals of time and the catalyst was separated by filtration. The quantitative determination of phenol was performed with a standard calorimetric method [30]. The mineralization of the substrate was monitored by determining the total organic carbon (TOC) content of the solution with a Carlo Erba TCM 480 analyzer. The formation of the main intermediates was investigated by high performance liquid chromatography (HPLC), using a Varian 9050 UV–Vis detector fitted with a Varian Model 9010 pump and an Econosphere C_{18} 3 μm 150 mm×4.66 mm i.d. column (Alltech). An acetonitrile–water solution (1:1 v/v) was used as the eluting solvent.

3. Results

3.1. Sample characterization

The X-ray diffraction patterns of the various powders have shown the contemporaneous presence of tungsten trioxide and tungsten disulfide in the samples [31,32]. Differences have been found among the diffractograms of the powders obtained by oxidation of WS_2 and those of the samples prepared by sulfidation of WO_3. As shown in Fig. 1, both the spectra of the oxidized and sulfidized samples are characterized by three narrow peaks at 2θ about 23–25°. Anyway, although the positions of these peaks are practically identical, their relative intensities are quite different. The ratios among the intensities of the peaks found for the sulfidized powders fit well with those of monoclinic WO_3 [31]. On the contrary, in the spectra of the oxidized samples, the presence of a strong and narrow peak followed by two much smaller ones, indicates a strong orientation of the WO_3 crystals along some preferential planes [29].

The X-ray spectra of the sulfidized supported samples revealed only the main peaks of WO_3 and WS_2. The intensities of these peaks were noticeably lower than those of the unsupported powders, indicating a bad crystallization and/or the presence of very small crystallites. It is worth noting that also the spectrum of the supported WO_3 precursor exhibited small peaks.

In Fig. 2 the diffuse reflectance spectra of two selected WO_3/WS_2 samples are reported and compared with those of the pure compounds. The spectra of the mixed powders are more or less similar to those of WO_3 or WS_2, according to whether the samples have been obtained, respectively by oxidation of the sulfide or by sulfidation of the oxide and depending on the extent of surface conversion of the starting chalcogenide.

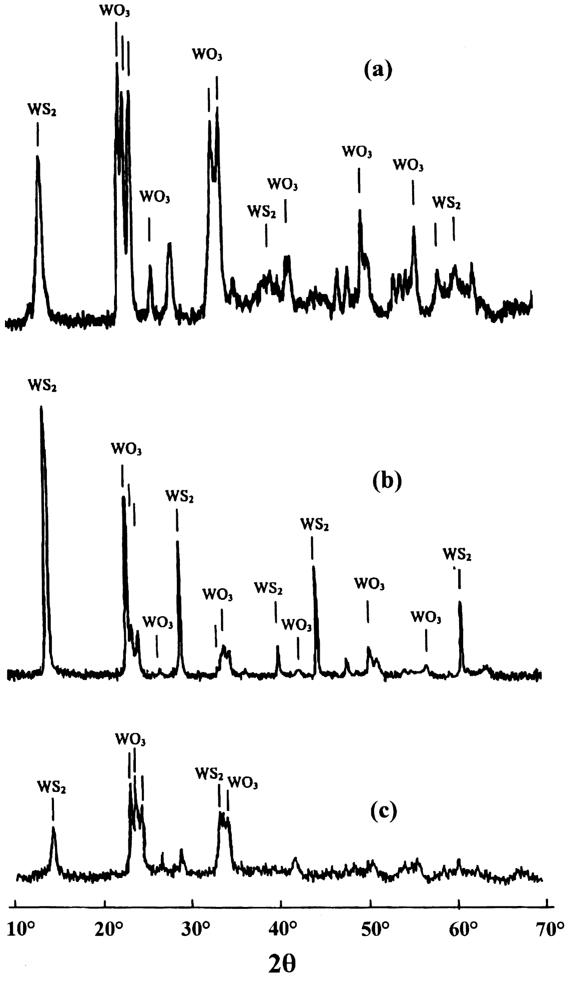

Fig. 1. X-ray diffraction patterns of various WO_3/WS_2 powders: (a) sulf/673/1.5/6; (b) ox/673/1.5/6; (c) sulf/673/1.5/10. The samples (a) and (c) were prepared, respectively from WO_3 (Carlo Erba) and 32 wt.% WO_3 on Al_2O_3.

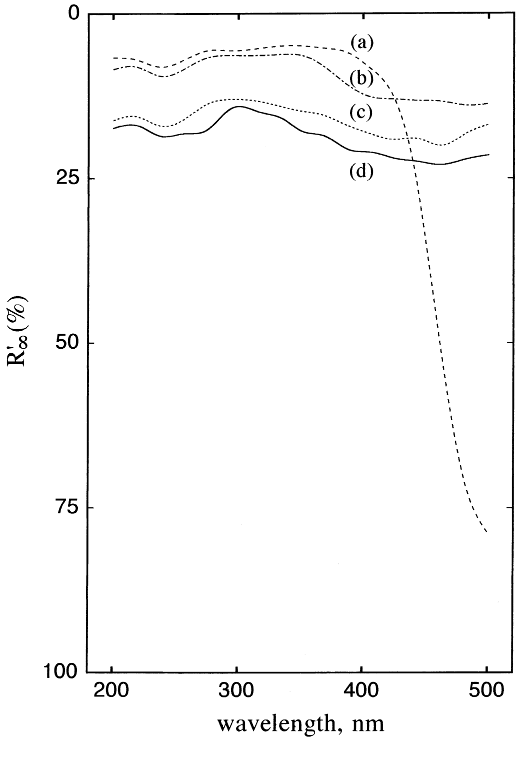

Fig. 2. Diffuse reflectance spectra of various samples: (a) WS_2; (b) WO_3; (c) ox/673/1.5/3; (d) sulf/673/1.5/3 prepared from WO_3 (Carlo Erba).

The specific surface areas of the various WO_3/WS_2 samples ranged between 2 and $6\,m^2\,g^{-1}$ and these values were not much different from those of WO_3 and WS_2 (2.4 and $1.7\,m^2\,g^{-1}$, respectively). The areas of the supported samples were significantly higher ($40–70\,m^2\,g^{-1}$) but the large surface area of alumina ($180\,m^2\,g^{-1}$) was dramatically reduced by the tungsten oxide loading.

XPS analysis has confirmed that the mixed samples contain the two chemical states of tungsten, W^{4+} as WS_2 and W^{6+} as WO_3, characterized by the W 4f binding energies [29]. The chemical states were the same independently of the precursor (WO_3 or WS_2) but the relative intensity of the two components changed according to the surface atomic composition. Discrepancies have been observed between the overall composition determined from chemical analysis and the surface composition obtained from XPS data. Table 1 reports the composition of some mixed samples in terms of molar fraction of WS_2.

Fig. 3 shows selected SEM micrographs of two different sulfidized samples, before and after reacting with H_2S. Sulfidation alters the macroscopic nature of the particles of WO_3 changing their initial irregular shape into well-defined needle-shaped crystals. Instead the size of the particles does not vary appreciably, in agreement with the surface area measurements. Fig. 3c and d, which refer to Al_2O_3-supported samples, reveal that the crystals of alumina are not uniformly covered by WO_3 or WO_3/WS_2. Further micrographs, not reported for the sake of brevity, have showed the existence of regions where significant amounts of tungsten chalcogenides were present.

EDX results have indicated a non-homogeneous distribution of WS_2 and WO_3 on the surface of the various mixed WO_3/WS_2 particles, revealing the presence of zones with a high content of WS_2 and zones richer in WO_3.

Table 1
Chemical composition of WO_3/WS_2 samples as molar fraction of WS_2[a]

Samples	$WS_2/(WS_2+WO_3)$	
	Chemical analysis	XPS
ox/673/1.5/6	0.79	0.47
ox/673/8/6	0.68	0.12
ox/673/2/3	0.68	0.42
sulf/673/1/10	0.32	0.47
sulf/873/1/10	0.77	0.65

[a] The accuracy on the values is estimated as ±10%.

3.2. Photocatalytic results

The photoreactivity experiments have shown that the rate of phenol disappearance depends on the amounts of WS_2 and WO_3 present in the mixed powders. Fig. 4 reports the photoconversion of phenol as C/C_o (C_o represents the initial concentration of organic substrate) versus the irradiation time, for some samples obtained by sulfidation of WO_3. The photoactivity of the samples was low when the content of WS_2 or WO_3 was small and reached a maximum value for a medium WS_2 overall composition. This behavior was observed for each set of powders, whatever the preparation method used.

In Fig. 5 the photoactivity of two WO_3/WS_2 samples is compared with that of pure WO_3 and WS_2. The data of the mixed systems refer to samples with about the same content of WS_2 (40%) but obtained, respectively by sulfidation of two different WO_3 powders. The results indicate that the mixed WO_3/WS_2 systems are much more active than the pure tungsten chalcogenides.

Fig. 6 shows the photooxidative disappearance of phenol in the presence of a supported mixed WO_3/WS_2 powder and the Al_2O_3-supported WO_3 precursor. The contemporaneous presence of WO_3 and WS_2 makes the mixed powder more efficient.

All the mixed samples are more photoactive than the corresponding mechanical mixtures. As shown in Fig. 7, although the composition of the physical mixture was similar to that of a sample obtained by sulfidation of WO_3, the behavior of this mixture was nearly identical to that displayed by WO_3, i.e. the semiconductor present in a larger amount.

As far as a comparison among the different sets of mixed samples is concerned, the photocatalytic results have indicated that the powders obtained by oxidation of WS_2 are generally the most efficient among the different mixed WS_2/WO_3 systems whereas the samples obtained by sulfidation of WO_3/Al_2O_3 have showed to be the least active.

The photoactivity of the various mixed WO_3/WS_2 powders actually depends on the surface content of WO_3 and WS_2 and not on the overall chemical compo-

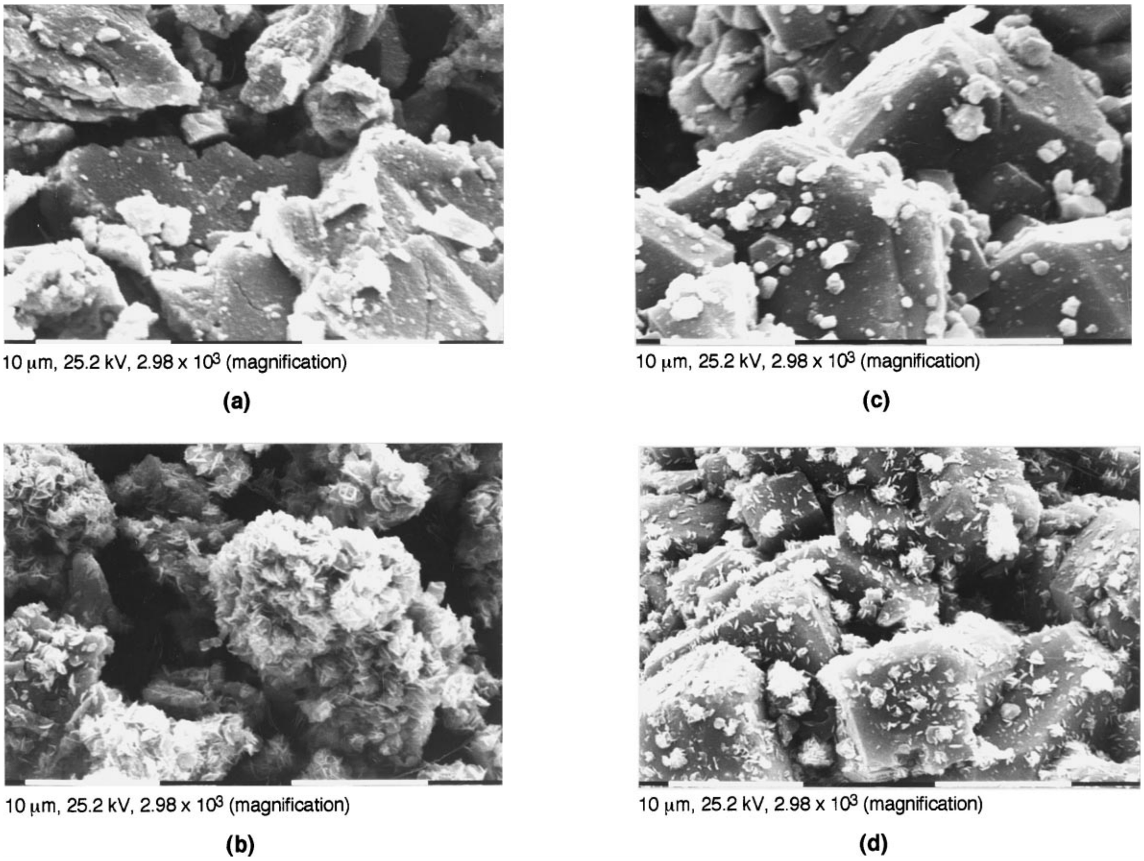

Fig. 3. Scanning electron micrographs of: (a) WO_3 (ex ammonium metatungstate); (b) sulf/673/1.5/10 prepared from WO_3 (ex ammonium metatungstate); (c) 55 wt.% WO_3 on Al_2O_3; (d) sulf/673/1.5/10 prepared from 55 wt.% WO_3 on Al_2O_3.

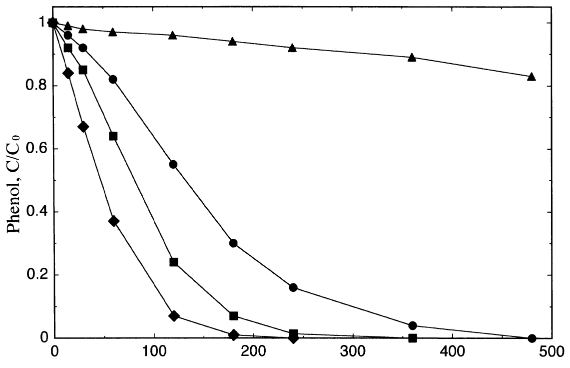

Fig. 4. Photocatalyzed conversion of phenol in the presence of various samples prepared by sulfidation of WO_3 (Carlo Erba): (■) 773/0.5/10; (◆) 673/1/10; (●) 673/3/10; (▲) 773/3/10.

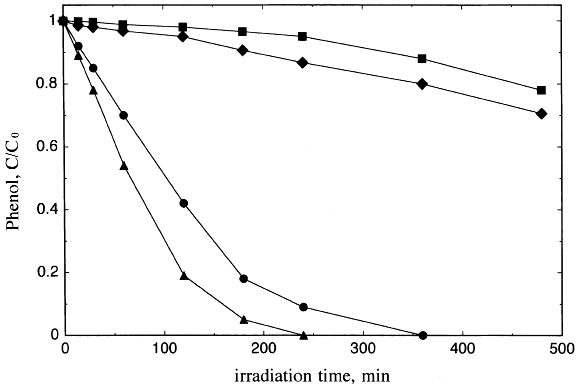

Fig. 5. Photocatalyzed conversion of phenol in the presence of various samples: (■) WS_2; (◆) WO_3; (▲) sulf/773/1/15 prepared from WO_3 (Carlo Erba); (●) sulf/823/1/10 prepared from WO_3 (ex ammonium metatungstate).

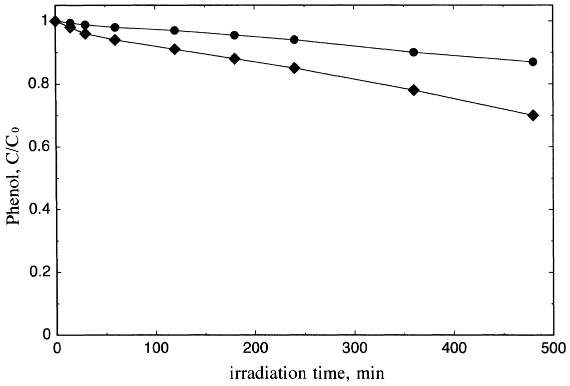

Fig. 6. Photocatalyzed conversion of phenol in the presence of supported samples: (●) 32 wt.% WO_3 on Al_2O_3; (◆) 32 wt.% WO_3 on Al_2O_3 sulfidized at 673 K for 1.5 h.

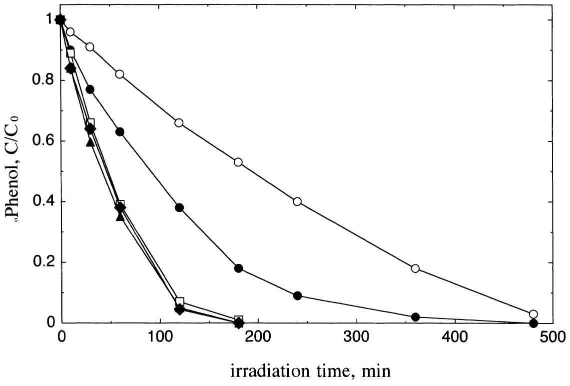

Fig. 8. Photocatalyzed conversion of phenol in the presence of various samples: (◆) ox/673/1.5/6; (●) ox/673/8/6; (▲) ox/673/2/3; (□) sulf/673/1/10; (○) sulf/873/1/10. The sulfidized samples were obtained starting from WO_3 (Carlo Erba).

sition. As shown in Fig. 8, the samples ox/673/1.5/6, ox/673/2/3 and sulf/673/1/10 which have comparable WS_2 surface values but different bulk content (see Table 1) have exhibited similar catalytic activities. Instead the samples ox/673/8/6 and sulf/873/1/10 have revealed to be much less active even if their bulk composition was very similar to that of the samples ox/673/2/3 and ox/673/1.5/6, respectively. It is worth noting that the highest photoactivities have been obtained when the surface molar fraction of WS_2 of the samples was about 0.5.

Phenol is scarcely mineralized to CO_2 and H_2O in the presence of the mixed WO_3/WS_2 powders [27,29]. Fig. 9 shows the variation of total organic carbon determined during the irradiation of two samples prepared following different procedures. The rate of phenol disappearance was very similar for both powders but a larger percentage of mineralization was obtained by using the oxidized sample.

The main compounds identified by HPLC were hydroquinone, cathecol and benzoquinone, i.e. the intermediate species usually detected during the heterogeneous photooxidation of phenol in the presence of TiO_2 [33]. The ratio of the intermediates changed depending on the WS_2 content of the samples [27].

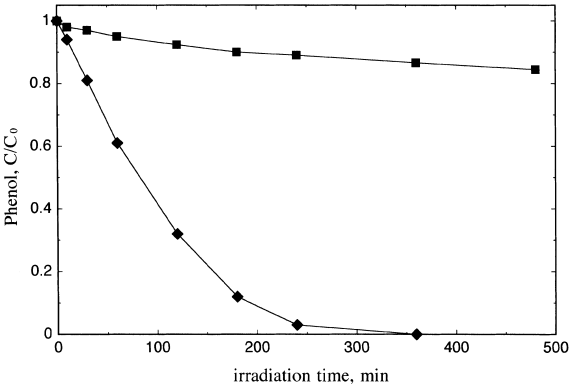

Fig. 7. Photocatalyzed conversion of phenol in the presence of various samples: (◆) sulf/673/1.5/10 prepared from WO_3 (ex ammonium meta-tungstate); (■) mechanical mixture WO_3/WS_2 (70/30 w/w).

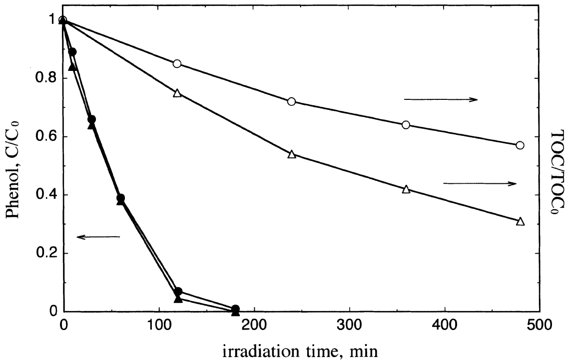

Fig. 9. Photocatalyzed conversion of phenol and variation of the total organic content with samples having the same surface composition (x_{WS_2}=0.47): (●) sulf/673/1/10 prepared from WO_3 (Carlo Erba); (▲) ox/673/1.5/6. The open symbols refer to the TOC data.

4. Discussion

While WO_3 and WS_2 are poor catalysts for the photooxidation of phenol, mixed polycrystalline WO_3/WS_2 powders have revealed an enhanced rate of disappearance of the organic substrate. As shown in previous works [27–29] the increased photoefficiency of these systems can be attributed to the contemporaneous presence of WO_3 and WS_2 in the same particle.

The photocatalytic behavior of the mixed powders can be explained considering the position of the energy levels of the two semiconductors. At pH=4.5 the conduction band of WS_2 (E_g=1.35 eV) is estimated to be at least 100 mV more cathodic than the conduction band of WO_3 (E_g=2.8 eV) while the valence band of WO_3 is significantly more positive than the corresponding band of WS_2 [27]. As shown in Fig. 10, when under UV illumination both semiconductors are simultaneously activated, the conduction band of WO_3 acts as a sink for the photogenerated electrons while a hole transfer occurs from the valence band of WO_3 to that of WS_2:

$$\mathrm{WS_2(e^- + h^+) + WO_3(\underline{e}^- + \underline{h}^+)} \\ \rightarrow \mathrm{WS_2(h^+ + \underline{h}^+) + WO_3(e^- + \underline{e}^-)}$$

The separation of electrons and holes in different semiconductor regions reduces the possibility of their wasteful recombination. The result of the vectorial transfer of charges is an increase of the lifetime of electrons and holes and consequently the efficiency of the interfacial charge transfer to the adsorbed substrate improves. The excess electrons on WO_3 are picked up by oxygen to yield the superoxide radical anion [6] while the excess holes on WS_2 ultimately oxidize the organic substrate.

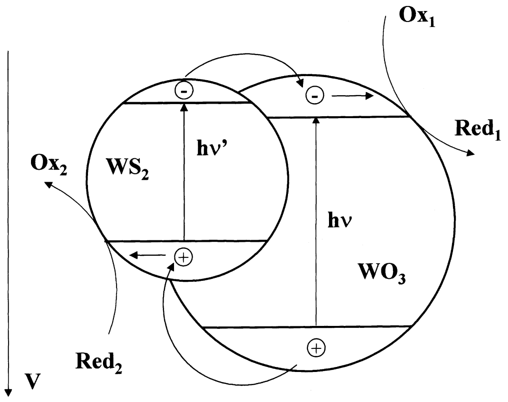

Fig. 10. Schematic diagram representing the charge transfer process in a WO_3/WS_2 system.

The simple coupling of two suitable semiconductors does not justify the enhanced photocatalytic efficiency of the mixed WO_3/WS_2 powders since no increase of the rate of phenol disappearance was revealed in the presence of mechanical mixtures of the two different chalcogenides. An intimate contact between WO_3 and WS_2 particles is necessary to achieve an efficient charge separation, in agreement with the results obtained by Ueno and coworkers [11–13] with supported mixed ZnS–CdS catalysts. Such intimate contact is permanently realized in the mixed systems where the particles are attached to each other whilst in the physically mixed powders there is only a temporary juxtaposition of two distinctly separated phases.

The photoreactivity results have shown that, independently of the preparation method (sulfidation of WO_3 or oxidation of WS_2), it is always possible to obtain photoactive samples. The rate of phenol photooxidation depends on the relative amounts of WO_3 and WS_2 present in the various samples, and, as shown in Fig. 8, is related to the surface composition of the particles rather than to the overall WO_3/WS_2 molar ratio.

The EDX analysis carried out on different locations of single mixed particles has revealed the presence of zones with different contents of WO_3 and WS_2. The surface of a WO_3/WS_2 particle can be imagined consisting of “islands” of WO_3 or WS_2 surrounded, respectively, by a “sea” of WS_2 or WO_3 [29]. The size and number of these “islands”, which are probably spread on the surface as the spots on a leopard skin, depends on the specific experimental conditions of preparation, i.e. temperature, time and starting amount of powder.

The coexistence of WO_3 and WS_2 areas on the single particles allow the formation of many heterotype “photochemical diodes” [34], i.e. microdevices where holes and electrons are separately injected into the adsorbed reactive species from different semiconducting regions. Parmon and coworkers [20,21] obtained systems with appropriate microheterojunctions upon contacting cadmium sulfide or zinc sulfide (or a mixed sulfide of these metals) with copper or silver sulfide. In this case the particles with such microheterojunctions were easily prepared by consecutive precipitation of the various semiconductor phases.

The efficiency of a mixed powder depends on the number of active sites present on the particles, i.e. on the number of microheterojunctions WO_3/WS_2. A WO_3/WS_2 system is generally more photoactive than the pure tungsten chalcogenides because the presence of few heterojunctions is sufficient to enhance the photooxidation rate of phenol [27]. The low photoactivity of a sample can be ascribed to a low surface content of WS_2 or WO_3. As confirmed by the XPS analysis, the highest photoactivity is obtained when the surface WS_2 molar fraction is near 0.5, probably corresponding to the maximum number of heterojunctions WS_2/WO_3 [29].

The powders obtained by oxidation of WS_2 are generally more efficient than those obtained by sulfidation of WO_3. The differences in photoactivity can be related to morphological and structural differences between the WO_3 phases present in the particles of the two mixed WS_2/WO_3 systems [29]. As shown by the XRD spectra, WO_3 obtained by oxidation of WS_2 is strongly orientated along some preferential planes. These planes are typical of WS_2 and consist of a monolayer of tungsten atoms intercalated between two parallel monolayers of sulfur atoms [35,36]. The substitution of the atoms of sulfur with those of oxygen does not cause a significant distortion of the WS_2 lattice, as confirmed by the small differences of the specific surface areas. Consequently, the surface of WO_3 will be mainly constituted by oxygen atoms which can establish an acid–base adsorption equilibrium with the phenol molecules dissolved in solution.

On the contrary, in the samples obtained by sulfidation of the commercial oxide, the phase WO_3 has a distorted ReO_3 structure, made up of distorted corner shared WO_6 octahedra [37]. In this case the surface consists of both oxygen and tungsten atoms and the formation of active sites involving oxygen atoms will be not particularly favored. The highest activity of the mixed powders obtained by oxidation of WS_2 can then be attributed to a more significant interaction between the organic substrate and the oriented WO_3 phase present on the surface of these samples.

Moreover, it is worth mentioning that the band gap value of the oriented WO_3 is slightly lower than that of commercial WO_3 [29] and this probably implies that the position of its energetic bands is more favorable for the vectorial displacement of electrons and holes between the particles of WO_3 and WS_2. Obviously other physico-chemical factors as geometry of the particles, surface texture or particle size distribution can play a significant role.

The photoreactivity of the supported samples was found to be very small although their BET surface areas were much higher than those of the unsupported powders. The low photoactivity can depend on the interaction between the WO_3 precursor and the support. As demonstrated by Chappell et al. [38] WO_3 interacts with the alumina when heated at 673 K or above. Tungsten reacts with surface hydroxyl groups to form oxotungsten species [39,40] and the dispersion of the WO_3 particles on Al_2O_3 causes a significant decrease in the surface area of the support, probably due to a blockage of the pores. The X-ray results indicate that the presence of Al_2O_3 hinders the growth of large crystals of WO_3 and this is in agreement with Laser Raman spectroscopy data revealing that below monolayer coverages (<25–30 wt.% WO_3 on Al_2O_3) tungsten oxide is present as a highly dispersed and amorphous state on the alumina surface [41,42].

The low efficiency of the supported WO_3/WS_2 powders could be due to the presence of high amounts of unreacted WO_3. In fact the WO_3/Al_2O_3 catalysts are difficult to sulfide [43] because of the stabilizing effect of W–O–Al links with the support [41] which polarizes the W–O bonds and make them less reactive. Nevertheless, the supported sulfidized samples are better catalysts than Al_2O_3-supported WO_3 because mixed WO_3/WS_2 particles are present on the surface.

As confirmed by the SEM observations, WO_3 is not uniformly distributed on the surface of the Al_2O_3 crystals. This is probably due to the impregnation method and causes significant differences in the rate of sulfidation. In the same reaction time, the smaller WO_3 particles are highly converted to WS_2 and consequently are much less active than the large particles containing a more favorable WO_3/WS_2 ratio. Moreover, the presence of Al_2O_3 could play a negative role preventing the electrical contact between WO_3 and WS_2.

5. Conclusions

Mixed WO_3/WS_2 systems have significantly higher photoactivities than the pure tungsten chalcogenides.

The enhanced efficiency has been attributed to the coupling of WO_3 and WS_2 which allows an efficient charge separation because of a vectorial transfer of electrons and holes from a semiconductor to another. Unlike other coupled semiconductor systems, the increase of the rate of phenol photooxidation is consistent with an intimate contact between the particles of WO_3 and WS_2 which are adjoined to each other. The photoactivity of the samples depends on the preparation method and the relative content of WO_3 and WS_2.

Acknowledgements

This work was financially supported by the Ministero dell'Università e della Ricerca Scientifica e Tecnologica (Roma). The authors thank Dr. A.M. Venezia for his invaluable assistance in the XPS measurements and for very helpful discussions.

References

[1] M. Schiavello (Ed.), Photocatalysis and Environment. Trends and Applications, Kluwer Academic Publishers, Dordrecht, 1988.
[2] E. Pelizzetti, N. Serpone (Eds.), Photocatalysis. Fundamentals and Applications, Wiley, New York, 1989.
[3] L. Spanhel, H. Weller, A. Henglein, J. Am. Chem. Soc. 109 (1987) 6632.
[4] K.I. Zamaraev, V.N. Parmon, in: E. Pelizzetti, M. Schiavello (Eds.), Photochemical Conversion and Storage of Solar Energy, Kluwer Academic Publishers, Dordrecht, 1991, p. 393.
[5] P.V. Kamat, B. Patrick, J. Phys. Chem. 96 (1992) 6829.
[6] N. Serpone, P. Maruthamuthu, P. Pichat, E. Pelizzetti, H. Hidaka, J. Photochem. Photobiol. A 85 (1995) 247.
[7] N. Serpone, E. Borgarello, M. Graetzel, J. Chem. Soc., Chem. Commun. (1984) 342.
[8] N. Serpone, E. Borgarello, E. Pelizzetti, M. Barbeni, Chim. Ind. 67 (1985) 318.
[9] N. Serpone, E. Borgarello, E. Pelizzetti, J. Electrochem. Soc. 135 (1988) 2760.
[10] P. Pichat, E. Borgarello, J. Disdier, M. Hermann, E. Pelizzetti, N. Serpone, J. Chem. Soc., Faraday Trans. I 84 (1988) 261.
[11] N. Kakuta, K.H. Park, M.F. Finlayson, A. Ueno, A.J. Bard, A. Campion, M.A. Fox, S.E. Webber, J.M. White, J. Phys. Chem. 89 (1985) 732.
[12] A. Ueno, N. Kakuta, K.H. Park, M.F. Finlayson, A.J. Bard, A. Campion, M.A. Fox, S.E. Webber, J.M. White, J. Phys. Chem. 89 (1985) 3828.
[13] J. Kobayashi, K. Kitaguchi, H. Tanaka, H. Tsuiki, A. Ueno, J. Chem. Soc., Faraday Trans. I 83 (1987) 1395.
[14] S. Hotchandani, P.V. Kamat, J. Phys. Chem. 96 (1992) 6834.
[15] J. Rabani, J. Phys. Chem. 93 (1989) 7707.
[16] A. Henglein, M. Gutierrez, H. Weller, A. Fojtik, J. Jirkovsky, Ber. Bunsenges. Phys. Chem. 93 (1989) 593.
[17] K.R. Gopidas, M. Bohorquez, P.V. Kamat, J. Phys. Chem. 94 (1990) 6435.
[18] L. Spanhel, A. Henglein, H. Weller, Ber. Bunsenges. Phys. Chem. 91 (1987) 1359.
[19] I. Bedja, P.V. Kamat, J. Phys. Chem. 99 (1995) 9182.
[20] Yu.A. Gruzdkov, E.N. Savinov, V.N. Parmon, Int. J. Hydrogen Energy 12 (1987) 393.
[21] E.N. Savinov, Yu.A. Gruzdkov, V.N. Parmon, Int. J. Hydrogen Energy 14 (1989) 1.
[22] D. Liu, P.V. Kamat, J. Phys. Chem. 97 (1993) 10769.
[23] K. Vinodgopal, P.V. Kamat, Environ. Sci. Technol. 29 (1995) 841.
[24] K. Vinodgopal, I. Bedja, P.V. Kamat, Chem. Mater. 8 (1996) 2180.
[25] C. Nasr, S. Hotchandani, W.Y. Kim, R.H. Schmehl, P.V. Kamat, J. Phys. Chem. 101 (1997) 7480.
[26] D. Liu, P.V. Kamat, J. Electroanal. Chem. 347 (1993) 451.
[27] A. Di Paola, L. Palmisano, M. Derrigo, V. Augugliaro, J. Phys. Chem. B 101 (1997) 876.
[28] A. Di Paola, L. Palmisano, M. Derrigo, V. Augugliaro, in: K. Rajeshwar, L.M. Peter, A. Fujishima, D. Meissner, M. Tomkiewich (Eds.), Proceedings of the Symposium on Photoelectrochemistry, The Electrochemical Society, Pennington, 1997, p. 321.
[29] A. Di Paola, L. Palmisano, A.M. Venezia, V. Augugliaro, J. Phys. Chem. B. 103 (1999) 8236.
[30] H.J. Taras, A.E. Greenberg, R.D. Hoak, M.C. Rand, Standard Methods for the Examination of Water and Wastewater, 13th Edition, American Public Health Association, Washington, DC, 1971.
[31] JCPDS file N. 5-0363.
[32] JCPDS file N. 8-237.
[33] V. Augugliaro, L. Palmisano, A. Sclafani, C. Minero, E. Pelizzetti, Toxicol. Environ. Chem. 16 (1988) 89.
[34] A.J. Nozik, Appl. Phys. Lett. 30 (1977) 567.
[35] H. Tributsch, Z. Naturforsch. 32a (1977) 972.
[36] J. Wilson, A.D. Yoffe, Adv. Phys. 18 (1969) 193.
[37] M. Schiavello, Chim. Ind. 61 (1979) 554.
[38] P.J.C. Chappell, M.H. Kibel, B.G. Baker, J. Catal. 110 (1988) 139.
[39] S.S. Chan, I.E. Wachs, L.L. Murrel, N. Dispenziers, Stud. Surf. Sci. Catal. 19 (1984) 259.
[40] Y. Iawasawa, in: D.D. Eley, P.W. Selwood, P.B. Weisz (Eds.), Advances in Catalysis, Vol. 35, Academic Press, New York, 1987, p. 187.
[41] L. Salvati, L.E. Makovsky, J.M. Stencil, F.R. Brown, D.M. Hercules, J. Phys. Chem. 85 (1981) 3700.
[42] L.L. Murrel, D.C. Grenoble, R.T.K. Baker, E.B. Prestridge, S.C. Fung, R.R. Chianelli, S.P. Cramer, J. Catal. 79 (1983) 203.
[43] B. Scheffer, P.J. Mangnus, J.A. Moulijn, J. Catal. 121 (1990) 18.